Backstepping Control of a Class of Continua of Linear Hyperbolic PDEs*

Jukka-Pekka Humaloja[1] and Nikolaos Bekiaris-Liberis[1]

***Abstract*— We develop a backstepping control design for a class of continuum systems of linear hyperbolic PDEs, described by a coupled system of an ensemble of rightward transporting PDEs and a (finite) system of m leftward transporting PDEs. The key analysis challenge of the design is to establish well-posedness of the resulting ensemble of kernel equations, since they evolve on a prismatic (3-D) domain and inherit the potential discontinuities of the kernels for the case of $n+m$ hyperbolic systems. We resolve this challenge generalizing the well-posedness analysis of Hu, Di Meglio, Vazquez, and Krstic to continua of general, heterodirectional hyperbolic PDE systems, while also constructing a proper Lyapunov functional.**

I. Introduction

Stabilization of large-scale systems of general, $n+m$ heterodirectional linear hyperbolic PDEs can be achieved via backstepping, see, for example, [1], [2], [3], [4], [5], [6], [7], [8]. Such large-scale systems of hyperbolic PDEs may be utilized to describe the dynamics of various systems with practical importance. In particular, they can be utilized to describe, traffic flow dynamics in large traffic networks [9], [10], [11], [12], as well as in multi-lane [13], [14] or multi-class traffic [15], [16]; blood flow dynamics in cardiovascular networks consisting of interconnected arterial segments [17], [18]; epidemics spreading dynamics in various geographical regions and among different age groups [19], [20], [21], [22]; dynamics of multi-phase flows in oil drilling applications [23]; and water networks dynamics [19], [24]. Complexity of computation of stabilizing backstepping kernels may, in general, grow with the number of PDE systems components [25], [26], which may, in fact, be alleviated constructing backstepping feedback laws based on continua PDE systems counterparts [25], [26]. Consequently, motivated by this and the practical significance of considering large-scale systems of hyperbolic PDEs, we address the problem of design of backstepping control laws for continua PDE systems, which are viewed as the continuum version of large-scale systems of $n+m$ heterodirectional linear hyperbolic PDEs. This constitutes the first step towards design of computationally tractable backstepping feedback laws for large-scale systems of $n+m$ hyperbolic PDEs.

The first result on backstepping stabilization of a class of continua of hyperbolic PDE systems was developed in [27], while a formal connection between the class of systems considered in [27] and the class of $n+1$ linear hyperbolic systems [28] (for large n), as well as the application of the control design originally developed for the continuum system to the large-scale counterpart, were made in [29], [26]. Therefore, besides [27] and [29], [26], the present paper is related to the results on backstepping stabilization of $n+m$ linear hyperbolic systems, see, for example, [1], [3], [4], [5], [6], [7], as well as to results in which PDE ensembles may arise as result of employment of Fourier transform, see, for example, [30] (that deals with parabolic PDEs). In addition, as the actual motivation for our developments is to address computational complexity of backstepping designs for large-scale hyperbolic systems, papers related to computation of backstepping kernels are also relevant, in particular, [31] that introduces a neural operators-based computation method, [32] that presents a late-lumping-based approach, and [33] that relies on power series representations of the kernels. Here we address the previously unattempted problem of backstepping control design for the continuum counterpart of a large-scale system of $n+m$ hyperbolic PDEs.

We start considering a continuum PDE system that corresponds to the $n+m$ hyperbolic system as $n\to\infty$ for which we employ the continuum PDE backstepping method. This gives rise to a continuum plus m kernel equations that are defined on a prismatic (3-D) domain that arises by continuating the triangular (2-D) domain of definition of the respective $n+m$ kernel equations. We establish well-posedness of the kernel equations treating them on each 3-D subdomain that is spanned along the direction of the ensemble variable from subdomains of the 2-D triangular space on which the kernels do not feature discontinuities. This allows us to then show continuity of the respective characteristic projections and to employ the successive approximations approach on each 3-D subdomain, thus generalizing the well-posedness results from [6], [7] and [27] for the $n+m$ and $\infty+1$ cases, respectively, to the case of a continuum plus m ($\infty+m$) kernels. Such a generalization is highly nontrivial and requires a delicate technical treatment as it inherits the technical intricacies of both going from $n+1$ to $n+m$ systems, in particular, the fact that the kernels may feature discontinuities, and going from a system with finite components to a continuum, in particular, having to deal with PDEs defined on 2-D domains instead of vector-valued 1-D PDEs. We establish exponential stability (in L^2) of the closed-loop system, constructing a Lyapunov functional. The theoretical results are validated on a numerical simulation example, for which the continuum kernels are derived in closed form.

*Funded by the European Union (ERC, C-NORA, 101088147). Views and opinions expressed are however those of the authors only and do not necessarily reflect those of the European Union or the European Research Council Executive Agency. Neither the European Union nor the granting authority can be held responsible for them.

[1]The authors are with the Department of Electrical and Computer Engineering, Technical University of Crete, Chania, Greece. Emails: jhumaloja@tuc.gr and nlimperis@tuc.gr.

Notation: We denote $E_c = L^2([0,1];L^2([0,1];\mathbb{R})) \times L^2([0,1];\mathbb{R}^m)$ and equip it with the inner product

$$\left\langle \left(\begin{smallmatrix} u_1 \\ \mathbf{v}_1 \end{smallmatrix}\right), \left(\begin{smallmatrix} u_2 \\ \mathbf{v}_2 \end{smallmatrix}\right) \right\rangle_{E_c} = \int_0^1 \left(\int_0^1 u_1(x,y)u_2(x,y)dy + \sum_{j=1}^m v_1^j(x)v_2^j(x) \right) dx. \quad (1)$$

Moreover, we say that a system is exponentially stable on E_c if, for any initial condition $z_0 \in E_c$, the (weak) solution $z \in C([0,\infty);E_c)$ of the system satisfies $\|z(t)\|_{E_c} \leq Me^{-ct}\|z_0\|_{E_c}$ for some constants $M,c>0$ that are independent of z_0. Finally, we denote by $\mathscr{T}$ the triangular set

$$\mathscr{T} = \left\{ (x,\xi) \in [0,1]^2 : 0 \leq \xi \leq x \leq 1 \right\}. \quad (2)$$

II. Stabilization of Continua $\infty+m$ Systems

A. Continua $\infty+m$ Systems of Hyperbolic PDEs

The considered class of continuum systems is of the form

$$u_t(t,x,y) + \lambda(x,y)u_x(t,x,y) = \int_0^1 \sigma(x,y,\eta)u(t,x,\eta)d\eta + \mathbf{W}(x,y)\mathbf{v}(t,x), \quad (3a)$$

$$\mathbf{v}_t(t,x) - \mathbf{M}(x)\mathbf{v}_x(t,x) = \int_0^1 \mathbf{\Theta}(x,y)u(t,x,y)dy + \mathbf{\Psi}(x)\mathbf{v}(t,x), \quad (3b)$$

with boundary conditions

$$u(t,0,y) = \mathbf{Q}(y)\mathbf{v}(t,0), \quad (4a)$$

$$\mathbf{v}(t,1) = \mathbf{U}(t), \quad (4b)$$

for almost every $y \in [0,1]$. Here we employ the matrix notation for $\mathbf{v},\mathbf{U},\mathbf{M},\mathbf{\Theta},\mathbf{\Psi},\mathbf{W}$ and $\mathbf{Q}$ for the sake of conciseness, that is, $\mathbf{v} = \left(v^j\right)_{j=1}^m$, $\mathbf{U} = \left(U^j\right)_{j=1}^m$, and the parameters are as follows.

Assumption 2.1: The parameters of (3), (4) are such that

$$\mathbf{M} = \operatorname{diag}(\mu_j)_{j=1}^m \in C^1([0,1];\mathbb{R}^{m\times m}), \quad (5a)$$

$$\mathbf{\Theta} = (\theta_j)_{j=1}^m \in C([0,1];L^2([0,1];\mathbb{R}^m)), \quad (5b)$$

$$\mathbf{\Psi} = (\psi_{i,j})_{i,j=1}^m \in C([0,1];\mathbb{R}^{m\times m}), \quad (5c)$$

$$\mathbf{W} = \begin{bmatrix} W_1 & \cdots & W_m \end{bmatrix} \in C([0,1];L^2([0,1];\mathbb{R}^{1\times m})), \quad (5d)$$

$$\mathbf{Q} = \begin{bmatrix} Q_1 & \cdots & Q_m \end{bmatrix} \in L^2([0,1];\mathbb{R}^{1\times m}), \quad (5e)$$

with $\lambda \in C^1([0,1]^2;\mathbb{R})$ and $\sigma \in C([0,1];L^2([0,1]^2;\mathbb{R}))$. Moreover, $\mu_m(x) > 0$ and $\lambda(x,y) > 0$ uniformly for all $x,y \in [0,1]$, and additionally

$$\min_{x\in[0,1]} \mu_j(x) > \max_{x\in[0,1]} \mu_{j+1}(x), \quad (6)$$

for all $j = 1,\ldots,m-1$. Finally, $\psi_{j,j} = 0$ for all $j = 1,\ldots,m$.[2]

[2]This comes without loss of generality, as such terms can be removed using a change of variables (see also, e.g., [6], [7]).

B. Continuum Backstepping Kernel Equations

The target system for the continuum Volterra backstepping transformation is chosen as

$$\alpha_t(t,x,y) + \lambda(x,y)\alpha_x(t,x,y) = \int_0^1 \sigma(x,y,\eta)\alpha(t,x,\eta)d\eta + \mathbf{W}(x,y)\boldsymbol{\beta}(t,x) + \int_0^1 \int_0^x C^+(x,\xi,y,\eta)\alpha(t,\xi,\eta)d\xi d\eta + \int_0^x \mathbf{C}^-(x,\xi,y)\boldsymbol{\beta}(t,\xi)d\xi, \quad (7a)$$

$$\boldsymbol{\beta}_t(t,x) - \mathbf{M}(x)\boldsymbol{\beta}_x(t,x) = \mathbf{G}(x)\boldsymbol{\beta}(t,0), \quad (7b)$$

with boundary conditions

$$\alpha(t,0,y) = \mathbf{Q}(y)\boldsymbol{\beta}(t,0), \quad (8a)$$

$$\boldsymbol{\beta}(t,1) = \mathbf{0}, \quad (8b)$$

for (almost) all $y \in [0,1]$, where $C^+ \in L^\infty(\mathscr{T};L^2([0,1]^2;\mathbb{R}))$, $\mathbf{C}^- \in L^\infty(\mathscr{T};L^2([0,1];\mathbb{R}^{1\times m}))$, and $\mathbf{G} \in L^\infty([0,1];\mathbb{R}^{m\times m})$ is strictly lower diagonal, i.e., $G_{i,j} = 0$ for all $i \leq j$. In order to map (3), (4) into (7), (8), we employ the following continuum Volterra transformation

$$\alpha(t,x,y) = u(t,x,y) \quad (9a)$$

$$\boldsymbol{\beta}(t,x) = \mathbf{v}(t,x) - \int_0^x \mathbf{L}(x,\xi)\mathbf{v}(t,\xi)d\xi - \int_0^x \int_0^1 \mathbf{K}(x,\xi,y)u(t,\xi,y)dyd\xi, \quad (9b)$$

where $\mathbf{L} \in L^\infty(\mathscr{T};\mathbb{R}^{m\times m})$ and $\mathbf{K} \in L^\infty(\mathscr{T};L^2([0,1];\mathbb{R}^m))$ are the backstepping kernels.[3]

Differentiating (9b) with respect to t and x, in order for (7) to hold, we obtain that $\mathbf{L}$ and $\mathbf{K}$ need to satisfy the following kernel equations (see [34, Appendix A] for the derivation)

$$\mathbf{M}(x)\mathbf{K}_x(x,\xi,y) - \mathbf{K}_\xi(x,\xi,y)\lambda(\xi,y) - \mathbf{K}(x,\xi,y)\lambda_\xi(\xi,y) = \mathbf{L}(x,\xi)\mathbf{\Theta}(\xi,y) + \int_0^1 \mathbf{K}(x,\xi,\eta)\sigma(\xi,\eta,y)d\eta, \quad (10a)$$

$$\mathbf{M}(x)\mathbf{L}_x(x,\xi) + \mathbf{L}_\xi(x,\xi)\mathbf{M}(\xi) + \mathbf{L}(x,\xi)\mathbf{M}'(\xi) = \mathbf{L}(x,\xi)\mathbf{\Psi}(\xi) + \int_0^1 \mathbf{K}(x,\xi,y)\mathbf{W}(\xi,y)dy, \quad (10b)$$

with boundary conditions

$$\mathbf{M}(x)\mathbf{L}(x,x) - \mathbf{L}(x,x)\mathbf{M}(x) + \mathbf{\Psi}(x) = 0, \quad (11a)$$

$$\mathbf{K}(x,x,y)\lambda(x,y) + \mathbf{M}(x)\mathbf{K}(x,x,y) + \mathbf{\Theta}(x,y) = 0, \quad (11b)$$

[3]We, in fact, show in Section III that $\mathbf{K}$ and $\mathbf{L}$ are piecewise continuous in $(x,\xi) \in \mathscr{T}$, so that evaluation along the boundaries of $\mathscr{T}$ is well-defined.

$$\mathbf{L}(x,0)\mathbf{M}(0)-\int_0^1\mathbf{K}(x,0,y)\lambda(0,y)\mathbf{Q}(y)dy=\mathbf{G}(x), \tag{11c}$$

for almost all $0\le\xi\le x\le 1$ and $y\in[0,1]$. More precisely, (11c) splits into two parts

$$\forall i\le j:\quad L_{i,j}(x,0)=\frac{1}{\mu_j(0)}\int_0^1 K_i(x,0,y)\lambda(0,y)Q_j(y)dy, \tag{12a}$$

$$\forall i>j:\qquad G_{i,j}(x)=\frac{1}{\mu_j(0)}\int_0^1 K_i(x,0,y)\lambda(0,y)Q_j(y)dy, \tag{12b}$$

where (12a) acts as a boundary condition for (10) and (12b) defines the nonzero elements of $\mathbf{G}$. Similarly to [6], [7], we also impose additional, artificial boundary conditions, to ensure the well-posedness of the kernel equations, as follows

$$\forall j<i:\qquad L_{i,j}(1,\xi)=l_{i,j}(\xi), \tag{13}$$

where the functions $l_{i,j}$ are chosen such that a C^0 compatibility condition is satisfied on $(x,\xi)=(1,1)$.[4] Thus, consistently with (11a), we impose

$$l_{i,j}(1)=-\frac{\psi_{i,j}(1)}{\mu_i(1)-\mu_j(1)}, \tag{14}$$

for all $j<i$. The well-posedness of the kernel equations (10)–(14) is considered in Section III.

C. Backstepping Feedback Law and Stability Result

The backstepping control law for $j=1,\dots,m$ is given by

$$U^j(t)=\int_0^1\int_0^1 K_j(1,\xi,y)u(t,\xi,y)dyd\xi+\int_0^1\sum_{i=1}^m L_{j,i}(1,\xi)v^i(t,\xi)d\xi, \tag{15}$$

which stabilizes (3), (4) by Theorem 2.2.

Theorem 2.2: Under Assumption 2.1, the control law (15) exponentially stabilizes the system (3), (4) on E_c.

Proof: We begin by noting that the target system (7), (8) has a well-posed solution on E_c due to the open-loop system (3), (4) being well-posed and (15) being a bounded state-feedback law from E_c to $\mathbb{R}^m$ (see [34, Rem. 1, Thm 1] for details). Now, we show that the (weak; see [29, Rem. 4.6] for details on the fact that existence and uniqueness of a weak solution suffices for making our Lyapunov-based arguments legitimate) solution to (7), (8) decays exponentially to zero, which by the invertibility of the transform (9) implies that the system (3), (4) under the control law (15) is exponentially stable. Inspired by [7, Prop. 2.1], the candidate Lyapunov functional with parameters $\delta,\mathbf{D}=\mathrm{diag}(D_1,\dots,D_m)>0$ is taken as

$$V(t)=\int_0^1\int_0^1 e^{-\delta x}\frac{\alpha^2(t,x,y)}{\lambda(x,y)}dydx+\int_0^1 e^{\delta x}\boldsymbol{\beta}^T(t,x)\mathbf{D}\mathbf{M}^{-1}(x)\boldsymbol{\beta}(t,x)dx. \tag{16}$$

Computing $\dot V(t)$ and integrating by parts in x gives

$$\begin{aligned}\dot V(t)=&\left[-e^{-\delta x}\|\alpha(t,x,\cdot)\|_{L^2}^2+e^{\delta x}\|\boldsymbol{\beta}(t,x)\|_{\mathbf{D}}^2\right]_0^1\\&-\delta\int_0^1\left(e^{-\delta x}\|a(t,x,\cdot)\|_{L^2}^2+e^{\delta x}\|\boldsymbol{\beta}(t,x)\|_{\mathbf{D}}^2\right)dx\\&+2\int_0^1\int_0^1\int_0^1 e^{-\delta x}\frac{\alpha(t,x,y)}{\lambda(x,y)}\sigma(x,\eta,y)\alpha(t,x,\eta)d\eta dydx\\&+2\int_0^1\int_0^1 e^{-\delta x}\frac{\alpha(t,x,y)}{\lambda(x,y)}\mathbf{W}(x,y)\boldsymbol{\beta}(t,x)dydx\\&+2\int_0^1\int_0^1\int_0^1\int_0^x e^{-\delta x}\frac{\alpha(t,x,y)}{\lambda(x,y)}C^+(x,\xi,y,\eta)\alpha(t,\xi,\eta)d\xi d\eta dydx\\&+2\int_0^1\int_0^1\int_0^x e^{-\delta x}\frac{\alpha(t,x,y)}{\lambda(x,y)}\mathbf{C}^-(x,\xi,y)\boldsymbol{\beta}(t,\xi)d\xi dydx\\&+\int_0^1 e^{\delta x}\boldsymbol{\beta}^T(t,x)\left(\mathbf{D}\mathbf{M}^{-1}(x)\mathbf{G}(x)+\mathbf{G}^T(x)\mathbf{M}^{-1}(x)\mathbf{D}\right)\boldsymbol{\beta}(t,0)dx,\end{aligned} \tag{17}$$

where $\|\cdot\|_{\mathbf{D}}^2=\langle\cdot,\mathbf{D}\cdot\rangle_{\mathbb{R}^m}$ denotes the $\mathbf{D}$-weighted inner product. Using the following bounds (that exist by Assumption 2.1 using Theorem 3.1; see [34, Lem. 7] for details)

$$m_\lambda=\min_{x,y\in[0,1]}\lambda(x,y),\quad m_\mu=\min_{j\in\{1,\dots,m\}}\min_{x\in[0,1]}\mu_j(x), \tag{18a}$$

$$M_\sigma=\max_{x\in[0,1]}\left\|\int_0^1\sigma(x,\cdot,\eta)d\eta\right\|_{L^2}, \tag{18b}$$

$$M_W=\max_{j=\{1,\dots,m\}}\max_{x\in[0,1]}\|W_j(x,\cdot)\|_{L^2}, \tag{18c}$$

$$M_{C^+}=\operatorname*{ess\,sup}_{(x,\xi)\in\mathscr{T}}\left\|\int_0^1 C^+(x,\xi,\cdot,\eta)d\eta\right\|_{L^2}, \tag{18d}$$

$$M_{C^-}=\max_{j\in\{1,\dots,m\}}\operatorname*{ess\,sup}_{(x,\xi)\in\mathscr{T}}\|C_j^-(x,\xi,\cdot)\|_{L^2}, \tag{18e}$$

$$M_G=\max_{i,j\in\{1,\dots,m\}}\operatorname*{ess\,sup}_{x\in[0,1]}\left|G_{ij}(x)\right|,\quad M_Q=\max_{j=1,\dots,m}\|Q_j\|_{L^2}, \tag{18f}$$

the boundary conditions (8), the Cauchy-Schwartz inequality, and $2\langle f,g\rangle_{L^2}\le\|f\|_{L^2}^2+\|g\|_{L^2}^2$ for any $f,g\in L^2$, we can estimate (17) as

$$\dot V(t)\le-\boldsymbol{\beta}^T(t,0)\left(\mathbf{D}-M_Q^2I_{m\times m}\right)\boldsymbol{\beta}(t,0)$$

[4] For the $\mathbf{L}$ kernels, a compatibility condition cannot (generally) be satisfied on $(x,\xi)=(0,0)$ due to (11a) and (11c), (11b).

$$
\begin{aligned}
&-\delta\int_0^1\left(e^{-\delta x}\|a(t,x,\cdot)\|_{L^2}^2+e^{\delta x}\|\boldsymbol{\beta}(t,x)\|_{\mathbf{D}}^2\right)dx\\
&+2\int_0^1 e^{-\delta x}\frac{M_\sigma+M_{C^+}}{m_\lambda}\|\alpha(t,x,\cdot)\|_{L^2}^2dx\\
&+\int_0^1 e^{-\delta x}\left(\frac{\|\alpha(t,x,\cdot)\|_{L^2}^2}{m_\lambda^2}+M_W^2\|\boldsymbol{\beta}(t,x)\|_{\mathbb{R}^m}^2\right)dx\\
&+\int_0^1 e^{-\delta x}\left(\frac{\|\alpha(t,x,\cdot)\|_{L^2}^2}{m_\lambda^2}+M_{C^-}^2\|\boldsymbol{\beta}(t,x)\|_{\mathbb{R}^m}^2\right)dx\\
&+mM_G\int_0^1 e^{\delta x}\boldsymbol{\beta}^T(t,x)\mathbf{D}\mathbf{M}^{-1}(x)\boldsymbol{\beta}(t,x)dx\\
&+\frac{mM_Ge^{\delta}}{\delta m_\mu}\boldsymbol{\beta}^T(t,0)\mathbf{F}\boldsymbol{\beta}(t,0),
\end{aligned}
\tag{19}
$$

where $\mathbf{F}=\operatorname{diag}(F_1,\dots,F_m)$ with

$$
F_j=\begin{cases}\sum_{i=j+1}^m D_i, & 1\le j\le m-1,\\ 0, & j=m,\end{cases}
\tag{20}
$$

where we employ the lower-triangular structure of $\mathbf{G}$ on the last two lines of (19). Now, $\dot V(t)$ can be guaranteed to be negative definite by choosing δ and $\mathbf{D}$ such that

$$
\delta>\max\left\{\frac{2m_\lambda(M_\sigma+M_{C^+})+2}{m_\lambda^2},\frac{M_W^2+M_{C^-}^2+mM_G}{m_\mu}\right\},
\tag{21a}
$$

$$
D_j>\left(1+(m-j)\frac{mM_Ge^{\delta}}{\delta m_\mu}\right)\max\left\{M_Q^2,1\right\},
\tag{21b}
$$

for all $j\in\{1,\dots,m\}$. More specifically, by defining

$$
c_V=\delta-\max\left\{\frac{2m_\lambda(M_\sigma+M_{C^+})+2}{m_\lambda^2},\frac{M_W^2+M_{C^-}^2+mM_G}{m_\mu}\right\},
\tag{22}
$$

we have

$$
\dot V(t)\le-\frac{c_V}{\max\left\{M_\mu,M_\lambda\right\}}V(t),
\tag{23}
$$

where

$$
M_\lambda=\max_{x,y\in[0,1]}\lambda(x,y),\quad M_\mu=\max_{j=\{1,\dots,m\}}\max_{x\in[0,1]}\mu_j(x),
\tag{24}
$$

which shows that the target system (7), (8) is exponentially stable. Thus, due to the invertibility of the transform (9), as (9b) is a Volterra equation for $\mathbf{v}$ (see [34, Lem. 8] for details), the control law (15) exponentially stabilizes (3), (4). ∎

III. Well-Posedness of the Continuum Kernels

Theorem 3.1: Under Assumption 2.1, the continuum kernel equations (10)–(14) have a well-posed solution $\mathbf{K}\in L^\infty(\mathscr{T};L^2([0,1];\mathbb{R}^m))$ and $\mathbf{L}\in L^\infty(\mathscr{T};\mathbb{R}^{m\times m})$. Moreover, the solution is piecewise continuous in $(x,\xi)\in\mathscr{T}$, where the set of discontinuities is of measure zero.

The proof is presented at the end of this section by utilizing the following lemmas.

Lemma 3.2 (Splitting kernels into continuity subdomains): The kernel equations (10) can be equivalently written in $L^\infty(\mathscr{T};L^2([0,1];\mathbb{R}^m)\times\mathbb{R}^{m\times m})$ as

$$
\begin{aligned}
&\mu_i(x)\partial_xK_i^p(x,\xi,y)-\partial_\xi K_i^p(x,\xi,y)\lambda(\xi,y)-K_i^p(x,\xi,y)\lambda_\xi(\xi,y)=\\
&\qquad\sum_{\ell=1}^m L_{i,\ell}^p(x,\xi)\theta_\ell(\xi,y)+\int_0^1 K_i^p(x,\xi,\eta)\sigma(\xi,\eta,y)d\eta,
\end{aligned}
\tag{25a}
$$

$$
\begin{aligned}
&\mu_i(x)\partial_xL_{i,j}^p(x,\xi)+\mu_j(\xi)\partial_\xi L_{i,j}^p(x,\xi)+\mu_j'(x)L_{i,j}^p(x,\xi)=\\
&\qquad\sum_{\ell=1}^m L_{i,\ell}^p(x,\xi)\psi_{\ell,j}(\xi)+\int_0^1 K_i^p(x,\xi,y)W_j(\xi,y)dy,
\end{aligned}
\tag{25b}
$$

for $1\le i\le p\le m$ and $j=1,\dots,m$, where $L_{i,j}^p,K_i^p$ denote the restrictions of the kernels to $\mathscr{T}_i^p$ and $\mathscr{P}_i^p$, respectively, defined as

$$
\mathscr{T}_i^p=\left\{(x,\xi)\in[0,1]^2:\rho_i^{p+1}(x)\le\xi\le\rho_i^p(x)\right\},
\tag{26a}
$$

$$
\mathscr{P}_i^p=\left\{(x,\xi,y)\in[0,1]^3:(x,\xi)\in\mathscr{T}_i^p\right\},
\tag{26b}
$$

where $\rho_i^{m+1}=0$ for all $i=1,\dots,m$ and

$$
\rho_i^p(x)=\phi_p^{-1}(\phi_i(x)),^5
\tag{27}
$$

for $1\le i\le p\le m$ with

$$
\phi_i(x)=\int_0^x\frac{ds}{\mu_i(s)},\qquad i=1,\dots,m.
\tag{28}
$$

The boundary conditions for (25) are given by

$$
\forall j\ne i:\quad L_{i,j}^i(x,x)=-\frac{\psi_{i,j}(x)}{\mu_i(x)-\mu_j(x)},
\tag{29a}
$$

$$
\forall i:\quad K_i^i(x,x,y)=-\frac{\theta_i(x,y)}{\lambda(x,y)+\mu_i(x)},
\tag{29b}
$$

$$
\forall i\le j:\quad L_{i,j}^m(x,0)=\frac{1}{\mu_j(0)}\int_0^1 K_i^m(x,0,y)\lambda(0,y)Q_j(y)dy,
\tag{29c}
$$

for $i,j=1,\dots,m$, with the artificial boundary conditions

$$
L_{ij}^p(1,\xi)=l_{i,j}(\xi),
\tag{30}
$$

for all $\xi\in[\rho_i^{p+1}(1),\rho_i^p(1)]$, $p=i,\dots,m$, and $1\le j<i\le m$. Moreover, the segmented kernels $K_i^p,L_{i,j}^p$ are subject to continuity conditions

$$
\forall i<p,\forall j\ne p:\qquad L_{i,j}^{p-1}(x,\rho_i^p(x))=L_{i,j}^p(x,\rho_i^p(x)),
\tag{31a}
$$

$$
\forall i<p:\quad K_i^{p-1}(x,\rho_i^p(x),y)=K_i^p(x,\rho_i^p(x),y),
\tag{31b}
$$

for all $i,j=1,\dots,m$, $i<p\le m$, and $x,y\in[0,1]$.

[5] These are the characteristic curves of (25b), which are strictly increasing in x and satisfy $0=\rho_i^{m+1}(x)<\rho_i^m(x)<\cdots<\rho_i^i(x)=x$ for all $1\le i\le p\le m$ and $x\in[0,1]$ by (6).

Proof: After splitting the kernels into the $\mathscr{T}_i^p$ and $\mathscr{P}_i^p$ segments, the transformation (9b) can be rewritten componentwise for $i = 1,\dots,m$ as

$$\beta_i(t,x) = v_i(t,x) - \sum_{j=1}^{m}\sum_{p=i}^{m}\int_{\rho_i^{p+1}(x)}^{\rho_i^p(x)} L_{i,j}^p(x,\xi)v_j(t,\xi)d\xi - \sum_{p=i}^{m}\int_{\rho_i^{p+1}(x)}^{\rho_i^p(x)}\int_0^1 K_i^p(x,\xi,y)u(t,\xi,y)dyd\xi. \quad (32)$$

The kernel equations (25) are obtained by inserting (32) to (7b) and integrating by parts once. In fact, the kernel equations (25) are exactly of the same form as (10) (written componentwise), and the boundary conditions (29), (30) correspond to (11a), (11b), (12a), and (13) along the respective boundaries (see Fig. 1 for an illustration of the $\mathscr{T}_i^p$ segments). Thus, the only difference to (10)–(13) are the continuity conditions (31), which arise due to the segmentation of $\mathscr{T}$ when differentiating (32) in x and integrating by parts once. ∎

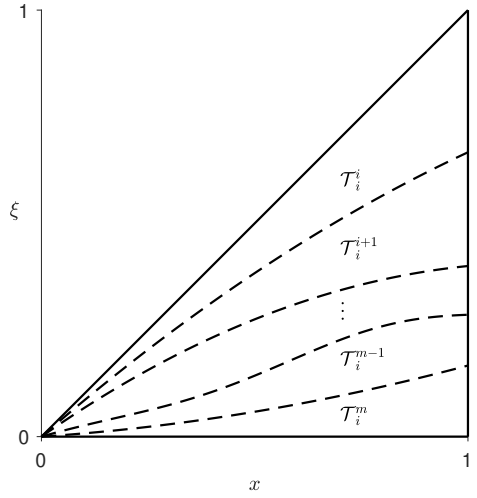

Fig. 1. Illustration of the segments $\mathscr{T}_i^p$ for $1 \le i \le p \le m$. The dashed lines are the characteristic curves $\xi = \rho_i^p(x)$ for $i < p \le m$.

The kernel equations (25) for $L_{i,j}^p$ and K_i^p on the segments $\mathscr{T}_i^p$ and $\mathscr{P}_i^p$ with boundary conditions (29)–(31) can be transformed into integral equations. In order to do this, in Lemma 3.3 we solve the characteristic projections for (25).

Lemma 3.3 (Continuity of characteristic projections): The characteristic projections for the kernel equations (25) are continuous on $\mathscr{T}_i^p$ and $\mathscr{P}_i^p$ for all $1 \le i \le p \le m$.

Proof: As λ is assumed to be in $C^1([0,1]^2;\mathbb{R})$, we can argue pointwise in $y \in [0,1]$ and solve the characteristic projections for the K_i^p kernels from the following Cauchy problems on $s \in [0, s_{i,p}^f(y)]$ for arbitrary, fixed $y \in [0,1]$ and $1 \le i \le p \le m$

$$\frac{d}{ds}\hat{x}_{i,p}(s,y) = -\mu_i(\hat{x}_{i,p}(s,y)), \quad (33a)$$

$$\frac{d}{ds}\hat{\xi}_{i,p}(s,y) = \lambda(\hat{\xi}_{i,p}(s,y),y), \quad (33b)$$

with boundary conditions $\hat{x}_{i,p}(0,y) = x, \hat{x}_{i,p}\left(s_{i,p}^f, y\right) = \hat{x}_{i,p}^f(y), \hat{\xi}_{i,p}(0,y) = \xi, \hat{\xi}_{i,p}\left(s_{i,p}^f, y\right) = \hat{\xi}_{i,p}^f(y)$. These Cauchy problems are of the same form as [27, (84)–(95)], by which, under Assumption 2.1, the solution to (33) tends towards the boundary $\xi = \rho_i^p(x)$, where it terminates at $s = s_{i,p}^f(y)$, corresponding to the boundary conditions (29c), (31b). Moreover, the characteristic projections solving (33) are continuous on each $\mathscr{P}_i^p$ by [27, Lem. 4].

The characteristic projections for the $L_{i,j}^p$ kernels are analogous to the $\ell_{i,j}^p$ kernels encountered in the $n+m$ case. Thus, this observation allows us to study continuity of the characteristic projections for the $L_{i,j}^p$ kernels similarly to [7, Thm A.1] and [6, Sect. VI.A.2]. To elaborate, for all $i,j = 1,\dots,m$ and $p = i,\dots,m$, the characteristic projections for the $L_{i,j}^p$ kernels are solutions of the following Cauchy problems on $s \in [0, s_{i,j,p}^f]$

$$\frac{d}{ds}\hat{x}_{i,j,p}(s) = \varepsilon_{i,j}\mu_i(\hat{x}_{i,j,p}(s)), \quad (34a)$$

$$\frac{d}{ds}\hat{\xi}_{i,j,p}(s) = \varepsilon_{i,j}\mu_j(\hat{\xi}_{i,j,p}(s)), \quad (34b)$$

with boundary conditions $\hat{x}_{i,j,p}(0) = x, \hat{x}_{i,j,p}\left(s_{i,j,p}^f\right) = \hat{x}_{i,j,p}^f$, $\hat{\xi}_{i,j,p}(0) = \xi, \hat{\xi}_{i,j,p}\left(s_{i,j,p}^f\right) = \hat{\xi}_{i,j,p,}^f$, and $\varepsilon_{i,j}$ defined as

$$\varepsilon_{i,j} = \begin{cases} 1, & i > j \\ -1, & i \le j \end{cases}. \quad (35)$$

For initial condition $(x,\xi) \in \mathscr{T}_i^p$, the location of the terminal condition $\left(\hat{x}_{i,j,p}^f, \hat{\xi}_{i,j,p}^f\right)$ depends on i,j,p and it is determined by the boundary conditions (29)–(31) (see [6, Figs. 4–6] for details). Thus, there exist unique, continuous characteristic projections as the solutions to (34) on $s \in [0, s_{i,j,p}^f]$, as every μ_i is continuously differentiable by Assumption 2.1. ∎

As the final step, we transform the kernel equations (25) into integral equations along the characteristic curves. By virtue of Lemma 3.3, we can then proceed with the method of successive approximations to obtain the unique continuous kernels $K_i^p, L_{i,j}^p$ solving (25)–(31) on each $\mathscr{T}_i^p$ by Lemma 3.4. Towards this end, integrating (25) along the characteristic curves and plugging in the boundary conditions (29)–(31) gives

$$K_i^p(x,\xi,y) - B_{i,p}^1\left(x_{i,p}^f(y), y\right) = -\int_0^{s_{i,p}^f(y)}\Big(K_i^p\left(\hat{x}_{i,p}(s,y), \hat{\xi}_{i,p}(s,y), y\right)\lambda_\xi\left(\hat{\xi}_{i,p}(s,y), y\right) + \int_0^1 K_i^p\left(\hat{x}_{i,p}(s,y), \hat{\xi}_{i,p}(s,y), \eta\right)\sigma\left(\hat{\xi}_{i,p}(s,y), \eta, y\right)d\eta + \sum_{\ell=1}^{m} L_{i,\ell}^p\left(\hat{x}_{i,j,p}(s), \hat{\xi}_{i,j,p}(s)\right)\theta_\ell\left(\hat{\xi}_{i,j,p}(s), y\right)\Big)ds, \quad (36a)$$

$$L^p_{i,j}(x,\xi) - B^2_{i,j,p}\left(\hat{\star}_{i,j,p}\left(s^f_{i,j,p}\right)\right) =$$

$$+\varepsilon_{i,j}\int_0^{s^f_{i,j,p}}\Big(\mu_j'(\hat{x}_{i,j,p}(s))L^p_{i,j}\left(\hat{x}_{i,j,p}(s),\hat{\xi}_{i,j,p}(s)\right)$$

$$-\int_0^1 K^p_i\left(\hat{x}_{i,j,p}(s),\hat{\xi}_{i,j,p}(s),y\right)W_j\left(\hat{\xi}_{i,j,p}(s),y\right)dy$$

$$-\sum_{\ell=1}^m L^p_{i,\ell}\left(\hat{x}_{i,j,p}(s),\hat{\xi}_{i,j,p}(s)\right)\psi_{\ell,j}\left(\hat{\xi}_{i,j,p}(s)\right)\Big)ds, \quad (36b)$$

where, for $j=1,\dots,m$ and $1\le i\le p\le m$,

$$B^1_{i,p}(x,y) = \begin{cases} -\frac{\theta_i(x,y)}{\lambda(x,y)+\mu_i(x)}, & p=i \\ K^{p-1}_i(x,\rho^p_i(x),y), & p>i \end{cases}, \quad (37a)$$

$$B^2_{i,j,p}(\star) = \begin{cases} -\frac{\psi_{i,j}(x)}{\mu_i(x)-\mu_j(x)}, & p=i, i\neq j \\ l^{(1)}_{i,j}(\xi), & p\ge i>j \\ L^{p-1}_{i,j}(x,\rho^p_i(x)), & p>i>j \\ L^{p-1}_{i,j}(x,\rho^p_i(x)), & i<p<j \\ \frac{1}{\mu_j(0)}\int_0^1 K^m_i(x,0,y)\lambda(0,y)Q_j(y)dy, & p=m, i\le j \\ L^{p+1}_{i,j}(x,\rho^{p+1}_i(x)), & i\le j\le p<m \end{cases}, \quad (37b)$$

denote the boundary conditions according to the terminal conditions of the characteristic projections solved in Lemma 3.3. The integral form (36) of the kernel equations can then be employed in constructing the series of successive approximations, by first inserting (arbitrary) initial guesses for K^p_i and $L^p_{i,j}$. The convergence of such successive approximations is established in Lemma 3.4.

Lemma 3.4 (Convergence of successive approximations): Let $j=1,\dots,m$ and $1\le i\le p\le m$ be arbitrary, and denote the sequences of successive approximations for the respective kernels K^p_i and $L^p_{i,j}$ corresponding to (36), (37) by $(K_\ell)_{\ell=0}^\infty$ and $(L_\ell)_{\ell=0}^\infty$, respectively, where we initialize K_0 and L_0 to zero. Then, the sequences of successive approximations converge such that

$$\lim_{\ell\to\infty}\max_{(x,\xi)\in\mathscr{T}^p_i}\left\|K_\ell(x,\xi,\cdot)-K^p_i(x,\xi,\cdot)\right\|_{L^2}=0, \quad (38a)$$

$$\lim_{\ell\to\infty}\max_{(x,\xi)\in\mathscr{T}^p_i}\left|L_\ell(x,\xi)-L^p_{i,j}(x,\xi)\right|=0. \quad (38b)$$

Proof: Denote the differences of successive approximations by $\Delta K_\ell = K_\ell - K_{\ell-1}$ and $\Delta L_\ell = L_\ell - L_{\ell-1}$ for $\ell\ge 1$. As K_0 and L_0 were initialized to zero, the terms in the sequences of successive approximations for $\ell\ge 1$ can be written as

$$K_\ell = \sum_{l=1}^\ell \Delta K_l, \qquad L_\ell = \sum_{l=1}^\ell \Delta L_l. \quad (39)$$

Now, the statement of the lemma is equivalent to the convergence of the series of differences (39) in the stated sense, which follows by showing that ΔK_ℓ and ΔL_ℓ, for any $\ell\ge 1$, satisfy

$$\|\Delta K_\ell(x,\xi,\cdot)\|_{L^2} \le M\frac{M^\ell_{K,L}(x-(1-\varepsilon)\xi)^\ell}{\ell!}, \quad (40a)$$

$$|\Delta L_\ell(x,\xi)| \le M\frac{M^\ell_{K,L}(x-(1-\varepsilon)\xi)^\ell}{\ell!}, \quad (40b)$$

uniformly on any $\mathscr{T}^p_i$, where $M, M_{K,L}>0$ are given by

$$M = M_B + \left(1+M^1_Q\right)\max_{x,y\in[0,1]}\max_{j=\{1,\dots,m\}}\frac{|\theta_j(x,y)|}{\lambda(x,y)+\mu_i(x)}, \quad (41a)$$

$$M_{K,L} = m(1+M^1_Q)\left(M^1_\lambda + M_\sigma + M_\theta\right)M^\varepsilon_\lambda + m\left(M^1_\mu + M_W + M_\psi\right)M^\varepsilon_\mu, \quad (41b)$$

where $M_B = \max\left\{M^1_B, M^2_B\right\}$ with

$$M^1_B = \max_{1\le i\neq j\le m}\max_{x\in[0,1]}\left|\frac{\psi_{i,j}(x)}{\mu_i(x)-\mu_j(x)}\right|, \quad (42a)$$

$$M^2_B = \max_{1\le j<i\le m}\max_{\xi\in[0,1]}\left|l^{(1)}_{i,j}(\xi)\right|, \quad (42b)$$

M_σ, M_W and M_λ, M_μ are given by (18b), (18c), and (24), respectively,

$$M^1_\lambda = \max_{x,y\in[0,1]}|\lambda_x(x,y)|, \quad M^1_\mu = \max_{j=\{1,\dots,m\}}\max_{x\in[0,1]}\left|\mu_j'(x)\right|, \quad (43a)$$

$$M_\theta = \sum_{j=1}^m \max_{x\in[0,1]}\|\theta_j(x,\cdot)\|_{L^2}, \quad M_\psi = \max_{x\in[0,1]}\|\Psi(x)\|_1, \quad (43b)$$

$$M^1_Q = \max_{j=\{1,\dots,m\}}\max_{y\in[0,1]}\frac{\lambda(0,y)}{\mu_j(0)}\|Q_j\|_{L^2}, \quad (43c)$$

where the parameter ε is taken such that

$$0<\varepsilon<1-\max_{1\le j<i\le m}\max_{x,\xi\in[0,1]}\frac{\mu_i(x)}{\mu_j(\xi)},^6 \quad (44)$$

and

$$M^\varepsilon_\lambda = \max_{i\in\{1,\dots,m\}}\max_{x,\xi,y\in[0,1]}\frac{1}{\mu_i(\xi)+(1-\varepsilon)\lambda(x,y)}, \quad (45a)$$

$$M^\varepsilon_\mu = \max_{i,j\in\{1,\dots,m\}}\max_{x,\xi\in[0,1]}\frac{-\varepsilon_{i,j}}{\mu_i(\xi)-(1-\varepsilon)\mu_j(x)}, \quad (45b)$$

where $\varepsilon_{i,j}$ is given in (35).

Due to linearity, the integral equations and boundary conditions for ΔK_ℓ and ΔL_ℓ are of the same form as (36) and (37), but with K and L replaced by ΔK_ℓ and ΔL_ℓ. Hence, the estimates (40) can be proved by induction based on (36) and (37). Firstly, the constant M (and the initialization of K_0, L_0 to zero) guarantees that the estimates (40) are satisfied for $\ell=1$, and for any arbitrary $\ell>1$ we have (40) by the induction assumption. To show that (40) then holds for $\ell\to\ell+1$, we insert the estimates (40), (43), and (18), into the integral equations for ΔK_ℓ and ΔL_ℓ. The following estimates are key

[6] Such ε exists by (6).

to the induction step, and can be proved analogously to [6, Lem. 6.2], for all $i,j=1,\dots,m$, $p=i,\dots,m$, and any $\ell\geq 1$

$$\int_0^{s^f_{i,p}(y)} \left(\hat{x}_{i,p}(s,y)-(1-\varepsilon)\hat{\xi}_{i,p}(s,y)\right)^\ell ds \leq M^\varepsilon_\lambda \frac{(x-(1-\varepsilon)\xi)^{\ell+1}}{\ell+1}, \tag{46a}$$

$$\int_0^{s^f_{i,j,p}} \left(\hat{x}_{i,j,p}(s)-(1-\varepsilon)\hat{\xi}_{i,j,p}(s)\right)^\ell ds \leq M^\varepsilon_\mu \frac{(x-(1-\varepsilon)\xi)^{\ell+1}}{\ell+1}, \tag{46b}$$

where $(x,\xi)\in\mathscr{T}_i^p$ is the (arbitrary) initial point of the respective characteristic curve on the $x\xi$-plane.

Using (46) together with (40) and the induction assumption, the induction step follows after similar computations as in [27, Sect. VI.C], albeit some additional care is required due to splitting the domain into the $\mathscr{T}_i^p$ segments, as some boundary conditions depend on ΔK_ℓ and ΔL_ℓ, which are unknown. However, as the boundary condition for ΔK_ℓ on every $\mathscr{T}_i^i$ is known (due to (37a)), we can solve (36a) first on every $\mathscr{T}_i^i$, and then utilize the obtained values to solve (36a) on $\mathscr{T}_i^{i+1}$, and so on, up to $\mathscr{T}_i^m$.[7] As the domain $\mathscr{T}$ is split into at most m segments, we need to solve (36a) at most m times over the different segments to compute the next successive approximation. Hence, an adequate value for $M_{K,L}$ corresponding to the estimate for ΔK_ℓ would be $m(M^1_\lambda+M_\sigma+M_\theta)M^\varepsilon_\lambda$, which gives the first term of (41b).

Deriving the estimate for ΔL_ℓ follows similar steps, where we again need to traverse through the segments $\mathscr{T}_i^p$ (depending also on j) to have known boundary conditions for the integral equation (36b). That is, for all $i\neq j$, we begin from $\mathscr{T}_i^i$ with known boundary condition on $\xi=x$ or $x=1$, and then utilize the continuity conditions in (37b) up to $\mathscr{T}_i^m$ if $i>j$, or up to $\mathscr{T}_i^{j-1}$ if $i<j$. For $i\leq j$, the remaining segments are reached by beginning from $\mathscr{T}_i^m$ with the boundary condition on $\xi=0$, and then utilizing the continuity conditions up to $\mathscr{T}_i^j$. As in the case of ΔK_ℓ, this results in having to solve (36b) at most m times, which results in the last term of (41b). Moreover, the boundary condition on $\xi=0$ depends on ΔK_ℓ, which can be dealt with using the estimate derived in the previous paragraph, which results in the remaining term $mM^1_Q(M^1_\lambda+M_\sigma+M_\theta)M^\varepsilon_\lambda$ in (41b). Thus, the estimate (40) follows by induction. Hence the series (39) and, equivalently, the sequences of successive approximations converge in the stated sense (38). ∎

Proof of Theorem 3.1: By Lemma 3.4, the sequences of successive approximations for any K_i^p and $L_{i,j}^p$ converge uniformly on $\mathscr{T}_i^p$ (K_i^p in the L^2 sense in y), which shows the existence (and well-posedness) of the solutions $K_i^p, L_{i,j}^p$ to the kernel equations (25)–(31). To conclude the proof of Theorem 3.1, we note that any two $\mathscr{T}_i^p$ and $\mathscr{T}_i^s$ with $p\neq s$ may only intersect along a common boundary $\xi=\rho_j^r(x)$ for $r=p$ or $r=s$ (if the segments are adjacent), which is a measure zero subset of $\mathscr{T}$. Thus, as the kernels $L_{i,j}^p$ and K_i^p are continuous on each $(x,\xi)\in\mathscr{T}_i^p$, and the intersections of these segments comprise a finite number of sets of measure zero, the discontinuities of the kernels K_i and $L_{i,j}$ may only occur in sets of measure zero.[8] In particular, the kernels $K_i, L_{i,j}$ solving (10)–(13) are uniquely determined by $K_i^p, L_{i,j}^p$ (K_i in the L^2 sense in y), almost everywhere on $\mathscr{T}$.

IV. Numerical Example and Simulation Results

Consider the parameters for $x,y,\eta\in[0,1]$

$$\lambda(x,y)=1,\quad \mu_1(x)=2,\quad \mu_2(x)=1, \tag{47a}$$

$$\sigma(x,y,\eta)=x^3(x+1)\left(y-\frac{1}{2}\right)\left(\eta-\frac{1}{2}\right), \tag{47b}$$

$$W_1(x,y)=W_2(x,y)=x(x+1)e^x\left(y-\frac{1}{2}\right), \tag{47c}$$

$$\theta_1(x,y)=-3y(y-1),\quad \theta_2(x,y)=-2y(y-1), \tag{47d}$$

$$\psi_{i,j}(x)=0,\quad i,j\in\{1,2\}, \tag{47e}$$

$$Q_1(y)=8\left(y-\frac{1}{2}\right),\quad Q_2(y)=-8(y-2), \tag{47f}$$

corresponding to an $\infty+m$ system for $m=2$. For these parameters, the solution to the continuum kernel equations (25), (29)–(31), where we choose $l_{2,1}=\psi_{2,1}=0$, is explicitly given by

$$K_1^1(x,\xi,y)=y(y-1), \tag{48a}$$

$$K_1^2(x,\xi,y)=e^{x-2\xi}y(y-1), \tag{48b}$$

$$K_2^2(x,\xi,y)=e^{2(x-\xi)}y(y-1), \tag{48c}$$

$$L_{1,1}^1(x,\xi)=L_{1,1}^2(x,\xi)=0, \tag{48d}$$

$$L_{1,2}^1(x,\xi)=0,\quad L_{1,2}^2(x,\xi)=-2e^{x-2\xi}, \tag{48e}$$

$$L_{2,1}^2(x,\xi)=0,\quad L_{2,2}^2(x,\xi)=-2e^{2(x-\xi)}, \tag{48f}$$

where $K_1^\star(\cdot,y), L_{1,1}^\star$, and $L_{1,2}^\star$ are defined on $\mathscr{T}_1^1=\{(x,\xi)\in[0,1]^2:\frac{1}{2}x\leq\xi\leq x\}$ and $\mathscr{T}_1^2=\{(x,\xi)\in[0,1]^2:\xi\leq\frac{1}{2}x\}$ for the respective superindex $\star=1,2$, while $K_2^2(\cdot,y), L_{2,1}^2$ and $L_{2,2}^2$ are defined on $\mathscr{T}_2^2=\mathscr{T}$, for each $y\in[0,1]$. Note the discontinuity in $L_{1,2}$ along $\xi=\frac{1}{2}x$.

For the simulation, the $\infty+m$ system with parameters (47) is approximated by a grid of 50 points in y and 256 points in x, where we use finite differences to approximate the differential operators. The resulting ODE is solved using `ode45` in MATLAB. The initial conditions are $u_0(x,y)=Q_1(y)+Q_2(y)$ and $v_0^1(x)=v_0^2(x)=1$ for all $x\in[0,1]$. The simulation results are shown in Figs. 2 and 3 for $t\in[0,5]$. In Fig. 2, the controls (15) are shown, demonstrating that they converge rapidly to zero. Fig. 3 shows the solution components $u(t,x,y)$ evaluated at $y=1$ and $v^1(t,x)$, which also converge rapidly to zero. Thus, based on Figs. 2 and 3, the control law (15) exponentially stabilizes the (initially unstable) $\infty+m$ system.

[7] Such a process is described in more detail in [5, Sect. 3.2].

[8] In fact, the discontinuities may only occur in the $L_{i,j}$ kernels for $1\leq i<j\leq m$ along the curves $\xi=\rho_i^j(x)$ due to (31).

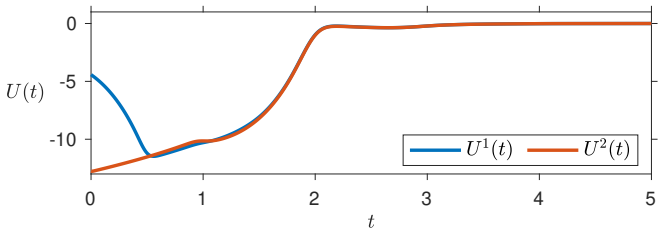

Fig. 2. The controls $U^1(t)$ and $U^2(t)$ based on the control law (15).

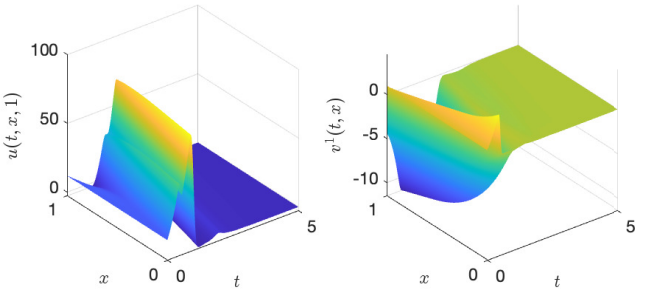

Fig. 3. The solution components $u(t,x,y)$ evaluated at $y=1$ and $v^1(t,x)$.

V. Conclusions

We introduced a backstepping control design methodology for a class of continua of hyperbolic PDE systems. Well-posedness of the derived kernel equations was established, together with exponential stability of the closed-loop system. The theoretical results were verified in numerical simulation. The application of the $\infty+m$ kernels to stabilization of large-scale $n+m$ systems is considered in the preprint [34].

References

[1] H. Anfinsen and O. M. Aamo, *Adaptive Control of Hyperbolic PDEs*. Springer, 2019.

[2] J. Auriol and D. Bresch-Pietri, "Robust state-feedback stabilization of an underactuated network of interconnected $n+m$ hyperbolic PDE systems," *Automatica*, vol. 136, Paper No. 110040, 2022.

[3] J. Auriol and F. Di Meglio, "Minimum time control of heterodirectional linear coupled hyperbolic PDEs," *Automatica*, vol. 71, pp. 300–307, 2016.

[4] J.-M. Coron, L. Hu, and G. Olive, "Finite-time boundary stabilization of general linear hyperbolic balance laws via Fredholm backstepping transformation," *Automatica*, vol. 84, pp. 95–100, 2017.

[5] F. Di Meglio, F. Bribiesca Argomedo, L. Hu, and M. Krstic, "Stabilization of coupled linear heterodirectional hyperbolic PDE-ODE systems," *Automatica*, vol. 87, pp. 281–289, 2018.

[6] L. Hu, F. Di Meglio, R. Vazquez, and M. Krstic, "Control of homodirectional and general heterodirectional linear coupled hyperbolic PDEs," *IEEE Trans. Automat. Control*, vol. 61, pp. 3301–3314, 2016.

[7] L. Hu, R. Vazquez, F. Di Meglio, and M. Krstic, "Boundary exponential stabilization of 1-dimensional inhomogeneous quasi-linear hyperbolic systems," *SIAM J. Control Optim.*, vol. 57, pp. 963–998, 2019.

[8] H. Ramirez, H. Zwart, and Y. L. Gorrec, "Exponential stability of boundary controlled port Hamiltonian systems with dynamic feedback," in *IFAC Workshop on Control of Systems Governed by Partial Differential Equation*, 2013, pp. 115–120.

[9] J. Friedrich, S. Göttlich, and M. Osztfalk, "Network models for nonlocal traffic flow," *ESAIM Math. Model. Numer. Anal.*, vol. 56, no. 1, pp. 213–235, 2022.

[10] S. Göttlich, M. Herty, S. Moutari, and J. Weissen, "Second-order traffic flow models on networks," *SIAM J. Appl. Math.*, vol. 81, pp. 258–281, 2021.

[11] L. Tumash, C. Canudas-de-Wit, and M. L. Delle Monache, "Multi-directional continuous traffic model for large-scale urban networks," *Transportation Research Part B: Methodological*, vol. 158, pp. 374–402, 2022.

[12] L. Zhang, H. Luan, Y. Lu, and C. Prieur, "Boundary feedback stabilization of freeway traffic networks: ISS control and experiments," *IEEE Trans. Control Syst. Technol.*, vol. 30, pp. 997–1008, 2022.

[13] M. Herty and A. Klar, "Modeling, simulation, and optimization of traffic flow networks," *SIAM J. Sci. Comput.*, vol. 25, pp. 1066–1087, 2003.

[14] H. Yu and M. Krstic, "Output feedback control of two-lane traffic congestion," *Automatica*, vol. 125, Paper No. 109379, 2021.

[15] M. Burkhardt, H. Yu, and M. Krstic, "Stop-and-go suppression in two-class congested traffic," *Automatica*, vol. 123, Paper No. 109381, 2021.

[16] R. Mohan and G. Ramadurai, "Heterogeneous traffic flow modelling using second-order macroscopic continuum model," *Phys. Lett.*, vol. 381, pp. 115–123, 2017.

[17] V. Bikia, "Non-invasive monitoring of key hemodynamical and cardiac parameters using physics-based modelling and artificial intelligence," Ph.D. dissertation, EPFL, 2021.

[18] P. Reymond, F. Merenda, F. Perren, D. Rufenacht, and N. Stergiopulos, "Validation of a one-dimensional model of the systemic arterial tree," *Am. J. Physiol. Heart Circ. Physiol.*, vol. 297, pp. H208–H222, 2009.

[19] G. Bastin and J.-M. Coron, *Stability and Boundary Sabilization of 1-D Hyperbolic Systems*. Birkhäuser/Springer, [Cham], 2016.

[20] L. Guan, C. Prieur, L. Zhang, C. Prieur, D. Georges, and P. Bellemain, "Transport effect of COVID-19 pandemic in France," *Annu. Rev. Control*, vol. 50, pp. 394–408, 2020.

[21] M. Iannelli, *Mathematical Theory of Age-structured Population Dynamics*. Giardini Editori e Stampatori in Pisa, 1995.

[22] C. Kitsos, G. Besancon, and C. Prieur, "High-gain observer design for a class of quasi-linear integro-differential hyperbolic systems-application to an epidemic model," *IEEE Trans. Automat. Control*, vol. 67, pp. 292–303, 2022.

[23] F. Di Meglio, G.-O. Kaasa, N. Petit, and V. Alstad, "Slugging in multiphase flow as a mixed initial-boundary value problem for a quasilinear hyperbolic system," in *American Control Conference*, 2011.

[24] A. Diagne, M. Diagne, S. Tang, and M. Krstic, "Backstepping stabilization of the linearized *Saint-Venant-Exner* model," *Automatica*, vol. 76, pp. 345–354, 2017.

[25] J.-P. Humaloja and N. Bekiaris-Liberis, "On computation of approximate solutions to large-scale backstepping kernel equations via continuum approximation," arXiv, 2406.13612, 2024.

[26] ——, "On stabilization of large-scale systems of linear hyperbolic PDEs via continuum approximation of exact backstepping kernels," in *IEEE Conference on Decision and Control*, 2024.

[27] V. Alleaume and M. Krstic, "Ensembles of hyperbolic PDEs: Stabilization by backstepping," *IEEE Trans. Automat. Control*, pp. 1–16, 2024.

[28] F. Di Meglio, R. Vazquez, and M. Krstic, "Stabilization of a system of $n+1$ coupled first-order hyperbolic linear PDEs with a single boundary input," *IEEE Trans. Automat. Control*, vol. 58, no. 12, pp. 3097–3111, 2013.

[29] J.-P. Humaloja and N. Bekiaris-Liberis, "Stabilization of a class of large-scale systems of linear hyperbolic PDEs via continuum approximation of exact backstepping kernels," arXiv, 2403.19455, 2024.

[30] R. Vazquez and M. Krstic, *Control of turbulent and magnetohydrodynamic channel flows*. Birkhäuser Boston, 2008.

[31] L. Bhan, Y. Shi, and M. Krstic, "Neural operators for bypassing gain and control computations in PDE backstepping," *IEEE Trans. Automat. Control*, 2024.

[32] J. Auriol, K. A. Morris, and F. Di Meglio, "Late-lumping backstepping control of partial differential equations," *Automatica*, vol. 100, pp. 247–259, 2019.

[33] R. Vazquez, G. Chen, J. Qiao, and M. Krstic, "The power series method to compute backstepping kernel gains: theory and practice," in *IEEE Conference on Decision and Control*, 2023, pp. 8162–8169.

[34] J.-P. Humaloja and N. Bekiaris-Liberis, "Backstepping control of continua of linear hyperbolic PDEs and application to stabilization of large-scale $n+m$ coupled hyperbolic PDE systems," arXiv, 2410.22067, 2024.